A MNEMONIC FOR THE LIPSHITZ–OZSVÁTH–THURSTON CORRESPONDENCE

ARTEM KOTELSKIY, LIAM WATSON, AND CLAUDIUS ZIBROWIUS

Abstract. When $\mathbf{k}$ is a field, type D structures over the algebra $\mathbf{k}[u,v]/(uv)$ are equivalent to immersed curves decorated with local systems in the twice-punctured disk [13]. Consequently, knot Floer homology, as a type D structure over $\mathbf{k}[u,v]/(uv)$, can be viewed as a set of immersed curves. With this observation as a starting point, given a knot K in S^3, we realize the immersed curve invariant $\widehat{HF}(S^3 \setminus \mathring{\nu}(K))$ [5] by converting the twice-punctured disk to a once-punctured torus via a handle attachment. This recovers a result of Lipshitz, Ozsváth, and Thurston [16] calculating the bordered invariant of $S^3 \setminus \mathring{\nu}(K)$ in terms of the knot Floer homology of K.

Recent work interprets relative versions of homological invariants in terms of immersed curves, including Heegaard Floer homology for manifolds with torus boundary [5], as well as link Floer homology [22], singular instanton knot homology [8], and Khovanov homology [13] for 4-ended tangles. In particular [13, Section 5] classifies type D structures over a quiver algebra associated with a surface with boundary in terms of immersed curves on this surface; compare [2, 5]. Perhaps the simplest algebra to illustrate these classification results is $\mathcal{R} = \mathbf{k}[u,v]/(uv)$ where $\mathbf{k}$ is a field. This algebra arises as the path algebra of a quiver that is associated with the decorated surface shown in Figure 1. And, it plays a central role in knot Floer homology; see [1], for instance.

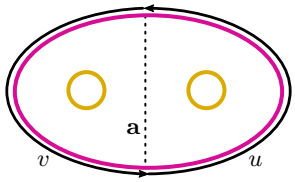

Figure 1. An arc system associated with the algebra $\mathcal{R}$.

Theorem 1. *Every type D structure over $\mathcal{R}$ is equivalent to an immersed curve (decorated with local systems) in the twice-punctured disk, which is unique up to regular homotopy (and equivalence of local systems).*

This is a special case of a theorem proved in [13, Section 5] appealing to techniques from [5] (see also [22]). We will review the algebraic objects in Section 1 and, without reproducing the proof in full, explain some key steps in this special case in Section 2. Theorem 1 gives rise to a graphical interpretation $\boldsymbol{\gamma}$ of ${}^{\mathcal{R}}CFK(Y,K)$, a variant of knot Floer homology which is a type D structure over $\mathcal{R}$. An explicit example of a curve $\boldsymbol{\gamma}$ in the twice-punctured disk is shown in Figure 2. This particular curve corresponds to the type D structure associated with the right-hand trefoil $T_{2,3}$ in S^3:

$$[\blacklozenge_1 \xleftarrow{u} \blacklozenge_2 \xrightarrow{v} \blacklozenge_3] = {}^{\mathcal{R}}CFK(S^3, T_{2,3})$$

Note that, while the local system in this example is trivial, these are easy to add to the picture in general, being equivalent to vector bundles over the curves in question (up to bundle isomorphism). There is an obvious handle attachment, identifying the two punctures in the disk, which yields a once-punctured torus. Denote this handle attachment by $\frown$ and consider the curve $\frown(\boldsymbol{\gamma})$. Note that, given a choice of meridian, this operation has an inverse that we will denote by $\multimap$. The term $\widehat{HF}(M)$ below refers to immersed curve in the once-punctured torus associated with a manifold M with torus boundary [5], which is equivalent to the bordered Heegaard Floer invariant of M [16].

AK is supported by an AMS-Simons travel grant. LW is supported by an NSERC discovery/accelerator grant and was partially supported by funding from the Simons Foundation and the Centre de Recherches Mathématiques, through the Simons-CRM scholar-in-residence program.

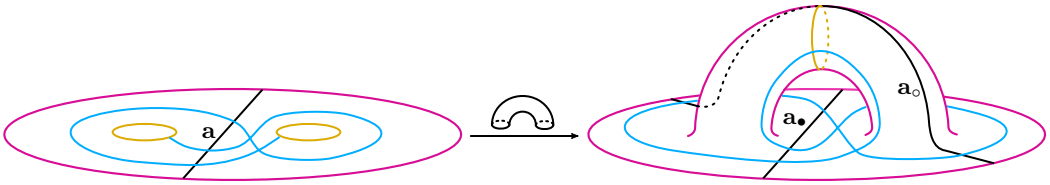

Figure 2. Adding a handle to the twice-punctured disk results in the once-punctured torus. This carries immersed curves to immersed curves; the immersed curve on the left corresponds to the type D structure ${}^{\mathcal{R}}CFK(S^3, T_{2,3}) = [\blacklozenge_1 \xleftarrow{u} \blacklozenge_2 \xrightarrow{v} \blacklozenge_3]$, which is carried to the curve $\widehat{HF}(M)$ where M is the trefoil exterior $S^3 \setminus \mathring{\nu}(K)$.

Theorem 2. *If $\boldsymbol{\gamma}$ is a curve representing the knot Floer invariant ${}^{\mathcal{R}}CFK(S^3, K)$, then $\curvearrowright(\boldsymbol{\gamma})$ is equivalent to $\widehat{HF}(M)$, where M is the exterior of the knot K. Conversely, given a meridian for $M = S^3 \setminus \mathring{\nu}(K)$, the curve $\curvearrowright\!\curvearrowleft\!\big(\widehat{HF}(M)\big)$ represents the knot Floer type D structure for K.*

Figure 2 illustrates this theorem in the case of the right-hand trefoil knot; the proof is given in Section 4. There is an apparent ambiguity in the statement, namely the number of twists (along the belt of the handle $\curvearrowright$) one adds to the non-compact component of the curve $\boldsymbol{\gamma}$. To resolve this, recall that the curve $\widehat{HF}(M) \subset \partial M$ is null-homologous in M [5, Sections 5 and 6]. So it remains to identify the once-punctured torus obtained after adding the handle with the boundary of the knot exterior (minus a small disk). We identify the arc $\mathbf{a}_\bullet$ from Figure 2 with the meridian μ, and the second arc $\mathbf{a}_\circ$ with a longitude λ of K. This pair provides a bordered structure, in the sense of Lipshitz–Ozsváth–Thurston [16]. Concerning the framing λ: On one hand there is a preferred choice given by the Seifert longitude λ_0, and the corresponding identification is depicted on the right of Figure 3. On the other hand, it is often simplest to work with the "blackboard framing", which simply joins the endpoints of $\boldsymbol{\gamma}$ without new twisting as they run over the handle, as in Figure 2. In general, this latter gives the $2\tau(K)$-framed longitude $\lambda_{2\tau} = 2\tau \cdot \mu + \lambda_0$, where the value $\tau(K)$ is the Ozsváth–Szabó concordance invariant (we describe how to extract this value below). This choice of longitude is illustrated on the left in Figure 3. These choices differ by Dehn twists along μ; note that in both cases $[\curvearrowright(\boldsymbol{\gamma})] = [\lambda_0]$ in homology. Different choices of twisting precisely correspond to different unstable chains appearing in [16, Theorems 11.26 and A.11], due to Lipshitz, Ozsváth, and Thurston, which Theorem 2 re-casts. This result generalizes to knots in arbitrary three-manifolds; see Section 5 for further discussion.

A graphical interpretation of the family of concordance homomorphism $\{\phi_i\}$ due to Dai, Hom, Stoffregen, and Truong [1] is given by Hanselman and the second author [7]. This can be read off the current picture: Denote by $\boldsymbol{\gamma}_0(K) \subset \boldsymbol{\gamma}(K)$ the non-compact curve in the twice-punctured disk associated with ${}^{\mathcal{R}}CFK(S^3, K)$. (The curve $\boldsymbol{\gamma}_0(K)$ is a concordance invariant [7, Proposition 2].) Orient $\boldsymbol{\gamma}_0(K)$ so that it leaves from the puncture recording the v^i coefficient maps; this is the left-hand puncture in Figure 1. Contracting the arc $\mathbf{a}$ to a point gives a wedge of annuli $A_v \vee A_u$, and the oriented segments of $\boldsymbol{\gamma}_0(K)$ around the left-hand puncture give a collection of homotopy classes in $\pi_1 A_v \cong \langle t \rangle$, where the generator t winds counterclockwise. As a result, given $\boldsymbol{\gamma}_0(K)$ with

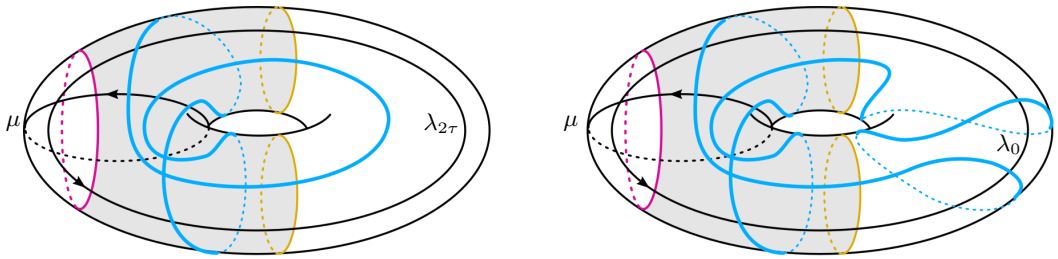

Figure 3. Choices of framing on the right-hand trefoil invariant: $2\mu + \lambda_0$ on the left and the preferred longitude λ_0 on the right. The resulting curve γ on the boundary of the trefoil exterior coincides with [6, Figure 9].

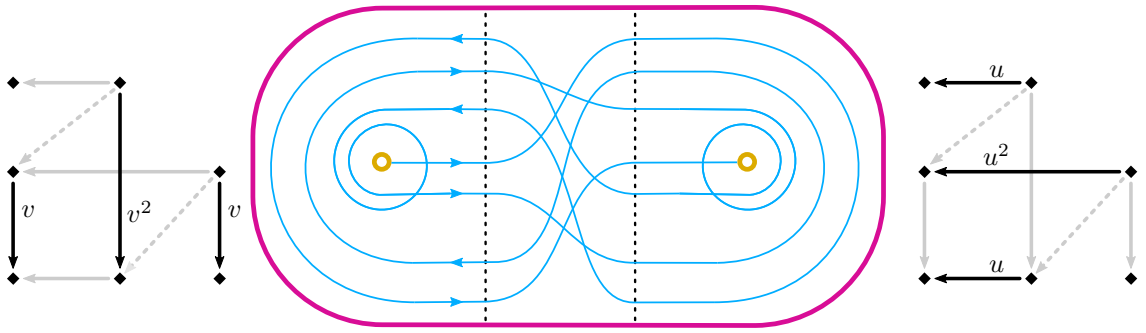

Figure 4. The curve associated with ${}^{\mathcal{R}}CFK(S^3,K)$ when K is the $(2,1)$-cable of the right-hand trefoil. The vertical and horizontal complexes are shown beside the relevant annuli; including the diagonal arrows describes the invariant over $\mathbf{k}[u,v]$. Applying Theorem 2 results in the curve-invariant in the torus, which can be compared with [7, Figure 1]. Orientating the curve as shown, we calculate $\phi_1(K)=0$, $\phi_2(K)=1$, and $\tau(K)=2$.

our choice of orientation we obtain $t^{n_1}t^{n_2}\cdots t^{n_k}$ for the k oriented segments winding around the puncture, and

$$\phi_i(K)=\sum_{n_j=\pm i}\operatorname{sign}(n_j)\qquad\qquad \tau(K)=\sum_{j=1}^{k}n_j$$

so that $\tau(K)$ is simply the winding number of $\boldsymbol{\gamma}$ around the left puncture. One can check that this gives $\tau(T_{2,3})=\phi_1(T_{2,3})=1$. A more complicated example is shown in Figure 4.

Relevant to concordance is the behaviour under connect sum. Denote by ${}_{\mathcal{R}}HFK(S^3,K)$ the knot Floer invariant obtained as a homology of a complex $CFK(S^3,K)$ freely generated over $\mathcal{R}$. In Section 6 we prove:

Theorem 3. *The knot Floer homology over $\mathcal{R}$ of a connected sum of two knots is equal to the wrapped Lagrangian Floer homology of the corresponding curves:*

$${}_{\mathcal{R}}HFK(S^3,mK\#K')\cong HF(\boldsymbol{\gamma}(K),\boldsymbol{\gamma}(K'))$$

1 Algebraic objects. Let $\mathcal{B}$ be a unital algebra over a field $\mathbf{k}$, with a subring of idempotents $\mathcal{I}$ being equal to $\mathbf{k}^n$. The object of interest is a chain complex over $\mathcal{B}$: let V be a finite dimensional left $\mathcal{I}$-module, and suppose further that we have a morphism of $\mathcal{I}$-modules

$$d\colon V\to\mathcal{B}\otimes V$$

satisfying the compatibility condition

$$(\mu\otimes\mathrm{id}_V)\circ(\mathrm{id}_{\mathcal{B}}\otimes d)\circ d=0$$

where μ denotes multiplication in $\mathcal{B}$. Then the pair (V,d) is a type D structure over $\mathcal{B}$.

A few comments: We work with left actions for consistency with [16]. Gradings are ignored for simplicity, but most objects and results in this paper—the algebra $\mathcal{R}$, type D structures over $\mathcal{R}$, curves associated with them, Theorems 1 and 3—have their bigraded analogues with respect to Alexander and δ-gradings; we refer the reader to [13, Sections 2 and 5]. Our type D structures will always be reduced, which means that $d(x)=\sum_i b_i\otimes y_i$ where none of the $b_i\in\mathcal{B}$ are invertible. This is justified by the fact that any type D structure is homotopy equivalent to a reduced one [13, Lemma 2.16].

Such algebraic structures appear naturally in a variety of settings. For example, given a knot K in S^3, the knot Floer invariant $HFK(S^3,K)$, due to Ozsváth–Szabó [17] and to Rasmussen [20], can be viewed as a $\mathbf{k}[u,v]$-module obtained as the homology of a chain complex $CFK(S^3,K)$ over the ring $\mathbf{k}[u,v]$ [21, Section 3]. This complex is freely generated as a module over this ring. As

such, it is natural to view $CFK(S^3,K)$ as a type D structure over $\mathbf{k}[u,v]$, which we denote by ${}^{\mathbf{k}[u,v]}CFK(S^3,K)$.

Given a type D structure over $\mathcal{B}$, a morphism of algebras $\mathcal{B}\to\mathcal{B}'$ gives rise to the induced type D structure. In particular, the quotient $\mathbf{k}[u,v]\to\mathbf{k}[u,v]/(uv)$ defines a truncated version of the knot Floer type D structure:

$$ {}^{\mathcal{R}}CFK(S^3,K) = {}^{\mathbf{k}[u,v]}CFK(S^3,K)\big|_{uv=0}$$

The associated module object ${}_{\mathcal{R}}CFK(S^3,K)$ (see [16, Lemma 2.20]) is the knot Floer complex freely generated over $\mathcal{R}$, which is studied in depth by Dai, Hom, Stoffregen, and Truong [1] and Ozsváth and Szabó [18]. A concise formula connecting the type D structure and the associated module object uses the box tensor product [15, Section 2.3.2 and Lemma 2.3.18]:

$$ {}_{\mathcal{R}}CFK(S^3,K) = {}_{\mathcal{R}}\mathcal{R}_{\mathcal{R}}\boxtimes {}^{\mathcal{R}}CFK(S^3,K)$$

We note that there are two type D structures obtained from ${}^{\mathcal{R}}CFK(S^3,K)$ by setting the appropriate variables equal to zero: the horizontal type D structure $C^{\mathbf{h}}$ and the vertical type D structure $C^{\mathbf{v}}$. For instance, in the case of the type D structure ${}^{\mathcal{R}}CFK(S^3,T_{2,3})$ (see Figure 2), we have

$$C^{\mathbf{h}} = [\blacklozenge_1 \xleftarrow{u} \blacklozenge_2 \quad \blacklozenge_3] \qquad\qquad C^{\mathbf{v}} = [\blacklozenge_1 \quad \blacklozenge_2 \xrightarrow{v} \blacklozenge_3]$$

As the type D structures are reduced, the isomorphisms $C^{\mathbf{h}}\big|_{u=0}\cong\widehat{HFK}(S^3,K)\cong C^{\mathbf{v}}\big|_{v=0}$ induce an isomorphism

$$\varphi\colon C^{\mathbf{h}}\big|_{u=0}\to C^{\mathbf{v}}\big|_{v=0}$$

We have:

Proposition 4. *The data specified by the triple* $(C^{\mathbf{h}},\ C^{\mathbf{v}},\ \varphi)$ *is equivalent to the type D structure* ${}^{\mathcal{R}}CFK(S^3,K)$.

Proof. This is immediate from the definitions, but also follows from the discussion in Section 2 outlining the proof of Theorem 1. □

2 Geometric objects. More generally, type D structures over $\mathcal{R}$ provide a useful toy model for illustrating the geometric classification described in [13]. A description of $\mathcal{R}$ as the path algebra of a quiver is given in Figure 1, where the quiver is extracted from the following geometric information: let D be a twice-punctured disk. We distinguish the boundary ∂D and fix the standard orientation on this circle induced by an orientation on the disk (with normal pointing out of the page), and choose an arc $\mathbf{a}$ properly embedded in $(D,\partial D)$ dividing D into a pair of annuli. The quiver, being a wedge of circles, is homotopic to the pair $(D,\mathbf{a})$; directions on the edges of the quiver are induced by the orientation on ∂D.

The choice of arc $\mathbf{a}$ is an example of an arc system on D, in the sense of [13, Section 5.1]. In general, an arc system, giving rise to an algebra $\mathcal{B}$, allows for a graphical representation of type D structures over $\mathcal{B}$ as sub-objects of the surface. These show up as train tracks in [5] and pre-curves in [13]; we describe them explicitly in the case of $\mathcal{R}$ and the twice-punctured disk D. It will be convenient to specify the annuli $D\setminus\mathbf{a}=A_v\sqcup A_u$; these annuli are called faces.

Let (V,d) be a type D structure over $\mathcal{R}$. Given a basis $\{x_1,\dots,x_n\}$ for V (as a vector space over $\mathbf{k}$, say), we can pick n distinct points on $\mathbf{a}$ and label these with the x_i. To describe the morphism d, suppose $b\otimes x_j$ is a summand of $d(x_i)$. Then, since b is a sum of polynomials, we may assume without loss of generality that b is λu^k or λv^k for some $\lambda\in\mathbf{k}$ and $k>0$. (The assumption that this power is non-zero comes from our restriction to reduced type D structures.) There are two cases: if $b=\lambda u^k$ then we connect x_i to x_j by an oriented arc immersed in A_u that winds algebraically k times in the positive direction; and if $b=\lambda v^k$ then we connect x_i to x_j by an oriented curve immersed in A_v that winds algebraically k times in the positive direction. In both cases the arc is decorated by the field coefficient λ, noting that when $\lambda=1$ our convention is to drop the label. In particular, when $\mathbf{k}$ is the two-element field, only the arcs are needed. To see that this information, having added all of the

curves describing d, can be viewed as an immersed train track in D, we simply require that every curve is perpendicular to $\mathbf{a}$ in a neighborhood of each x_i. An explicit example is given in Figure 5.

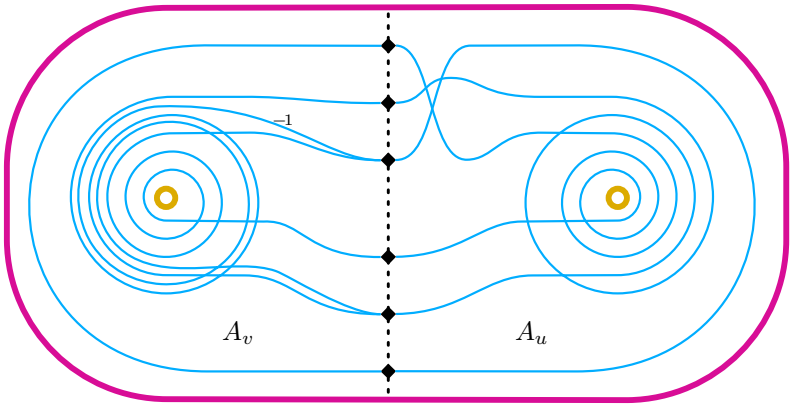

Figure 5. A sample train track representation of a type D structure over $\mathcal{R}$. Note that every curve segment is oriented so that it runs counter-clockwise around a puncture, so this orientation is omitted. Similarly, unlabeled edges (of which there are all but one in this example) carry the decoration $\lambda = 1$.

These train tracks can be put into a simple form that makes them easier to manage: we require that they are simply faced in the sense of [13, Definition 5.9]. In the present setting, this amounts to expressing

$$D = A_v \cup_{\mathbf{a}\times\{1\}} \left(\mathbf{a} \times [-1,1]\right) \cup_{\mathbf{a}\times\{-1\}} A_u$$

and requiring that the train track restricted to A_u and to A_v describes a type D structure over $\mathbf{k}[u]$ and $\mathbf{k}[v]$, respectively, with the property that each x_i connects to at most one x_j. For an illustration see Figure 6. All of the interesting switching is confined to the strip $\mathbf{a} \times [-1,1]$, which amounts to a graphical interpretation (reading from right to left) of an isomorphism $\varphi\colon V_u \to V_v$, where V_v and V_u are the underlying vector spaces associated with the type D structure in each face. As such, the general fact that we can restrict to simply faced train tracks (see [13, Proposition 5.10]) boils down to the fact that type D structures over $\mathcal{R}$ admit vertically and horizontally simplified bases [16, Definition 11.23]—though not necessarily one that is simultaneously vertically and horizontally simplified, whence the choice of isomorphism. This last assertion explains the presence of φ; compare Proposition 4.

We make some comments about our conventions, reviewing [13, Section 5.6]. The object appearing in the strip $\mathbf{a} \times [-1,1]$ represents an invertible matrix, where the i^{th} column records the edges leaving the point labeled x_i on $\mathbf{a}\times\{-1\}$ ($\mathbf{a}$ is oriented from top to bottom in our figures, so that $\{-1\}$ is the right most edge of the strip). Using the row-reduction algorithm, this matrix can be factorized into elementary matrices corresponding to three geometric sub-objects, as shown in Figure 7. These sub-objects differ from the ones in [5], where the coefficients are restricted to the two-element field. New in the context of general fields are the non-zero coefficients $\lambda \in \mathbf{k}$, recorded on the crossover switches (these correspond to crossover arrows from [5]), as well as the passing loops, which introduce coefficients at various points. The main point is that when two coefficients appear consecutively on one edge connecting the source and the target, the coefficients multiply, while if two edges share a common source and a common target, the coefficients on those edges add. We note that the geometric objects contain not only the information encoding φ (reading from right-to-left) but also the information about the inverse φ^{-1} (reading from left-to-right). As such, some of the data in the crossover switches and in the passing loops is superfluous. In particular, to simplify pictures below, we will record only the arrows running from right-to-left.

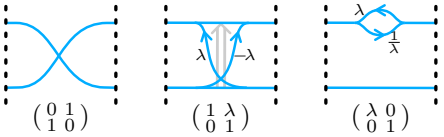

Figure 7. A crossing, a crossover switch, and a passing loop, each with the elementary matrix they represent by reading paths right-to-left.

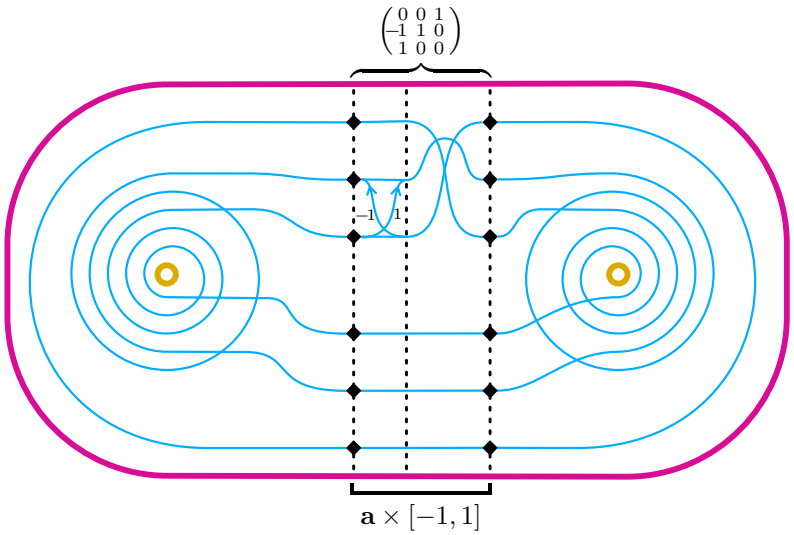

Figure 6. Expressing the train track from Figure 5 as a simply faced precurve. The isomorphism described can be read off the tracks in $\mathbf{a} \times [-1, 1]$ from right to left; in the present setting the resulting matrix block-decomposes into two 3×3 parts, of which one is shown and the other is the identity matrix.

It is convenient to put the matrix representing φ into a normal form, and interpret this geometrically. For example, the matrix $\left(\begin{smallmatrix} \lambda & 1 \\ 1 & 0 \end{smallmatrix}\right)$ may be expressed as

$$\left(\begin{smallmatrix} 1 & \lambda \\ 0 & 1 \end{smallmatrix}\right)\left(\begin{smallmatrix} 0 & 1 \\ 1 & 0 \end{smallmatrix}\right) = \left(\begin{smallmatrix} 1 & 0 \\ \lambda^{-1} & 1 \end{smallmatrix}\right)\begin{pmatrix} \lambda & 0 \\ 0 & -\lambda^{-1} \end{pmatrix}\left(\begin{smallmatrix} 1 & \lambda^{-1} \\ 0 & 1 \end{smallmatrix}\right)$$

An alternative is to view this equality in pictures, as shown in Figure 8.

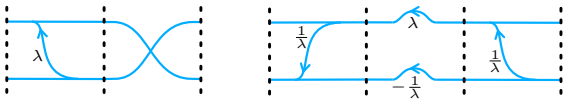

Figure 8. Two equivalent sections of track.

This is a form that can be obtained in general, and corresponds to the **LPU** form for matrices: Any invertible matrix can be written as a product of a **L**ower triangular matrix, a **P**ermutation matrix (which may be multiplied, additionally, by a diagonal matrix to change coefficients), and an **U**pper triangular matrix. Geometrically, this expresses the train track in the region $\mathbf{a} \times [-1, 1]$ with downward arrows on the left, a permutation in the middle, and upward arrows on the right. A complete list of geometric moves corresponding to different factorizations into elementary matrices is given in [13, Figure 23]. The described process is illustrated by transitioning from Figure 6 to Figure 10.

The reason this form is useful is that it allows us to remove arrows and simplify. This is possible in general, by appealing to an algorithm given in [5], and ultimately gives rise to the proof of Theorem 1; see [13, Section 5] for details. The main point is that arrows winding counterclockwise around a puncture can be removed. Namely, suppose there is an arrow near an edge of the strip $\mathbf{a} \times [-1, 1]$ that, when pushed into the relevant annulus, runs counterclockwise between curve-segments with different amounts of wrapping. Then there is a homotopy equivalence that produces a new train

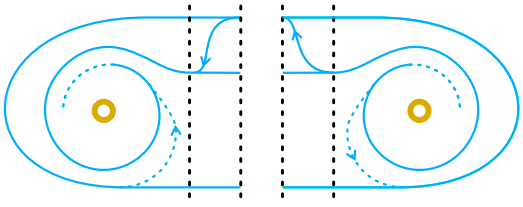

Figure 9. Arrows running counterclockwise can be removed.

track—with the counterclockwise arrow removed—representing the same type D structure; see Figure 9. This is described in detail in [13, Lemma 5.11]. The result of this procedure, applied to the example described in Figure 10, is shown in Figure 11.

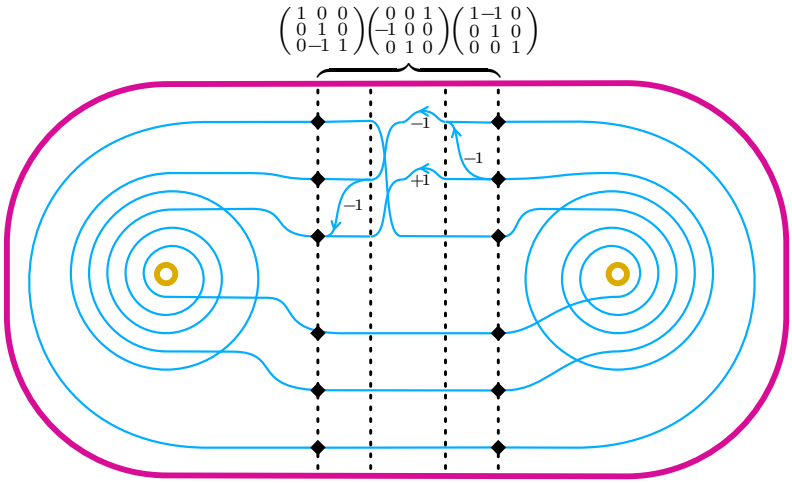

Figure 10. Modifying the train track from Figure 6 according to an **LPU** decomposition of the matrix.

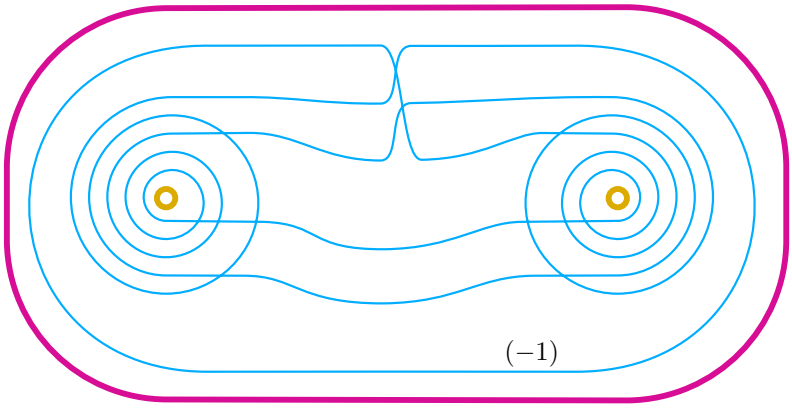

Figure 11. Modifying the train track from Figure 10 by removing the counter-clockwise arrows. This produces an immersed curve—an object that is equivalent to the train track from Figure 5, and which carries a 1-dimensional local system with automorphism that multiplies by −1.

Recall that a local system over an immersed curve is a vector bundle over the curve. In general, all of our curves carry local systems, but when the associated bundle is one-dimensional and trivial we drop it from the notation. When working with signs, one-dimensional local systems are quite common as the coefficients along any given curve component multiply. Of course, non-compact curves do not carry interesting local systems since all vector bundles are trivial in this case. On the other hand, for compact curves it should be clear from the construction described above where a local system can arise: If two compact curves run parallel, then a crossover switch running between them cannot be removed by a chain isomorphism of type D structures. In general, local systems provide a clean way of presenting the relevant invariants, while the formalism expressing curves with local systems in terms of train tracks gives a concrete means of working with these objects. An example is shown in Figure 12; notice that, by replacing φ with φ^{-1} in this example, one can obtain a vertically simplified basis or a horizontally simplified basis, but not both simultaneously. It appears to still be an open question if such phenomena arises for invariants associated with knots; see [12, Remark 2.9].

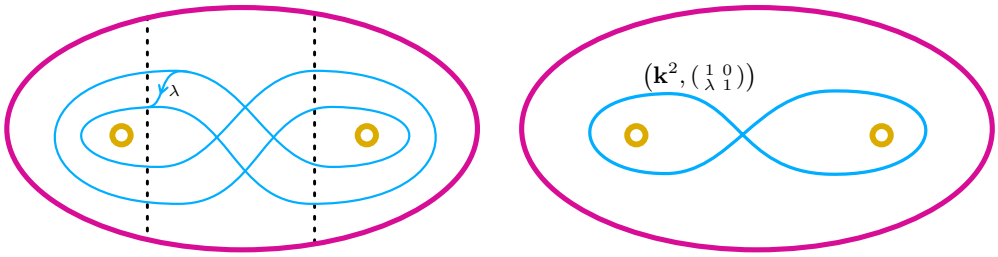

Figure 12. An arrow that cannot be cancelled gives rise to a non-trivial local system.

3 Adding a handle. We now introduce the second algebra: the extended torus algebra $\widetilde{\mathcal{A}}$. This algebra is introduced in [5], and is also the algebra arising naturally in our setting. By construction, the map $\frown$ takes the twice-punctured disk to the once-punctured torus T. An arc system for the latter is shown in Figure 13, from which the associated quiver can be extracted—as before we contract the arcs to the quiver vertices. Consulting Figure 14, note that $\mathbf{a}_\bullet$ is identified with the meridian μ and $\mathbf{a}_\circ$ is identified with the choice of longitude λ. With this arc system we associate an algebra $\widetilde{\mathcal{A}}$. Analogous to the relation $uv = 0$ from Figure 2, the algebra $\widetilde{\mathcal{A}}$ has relations

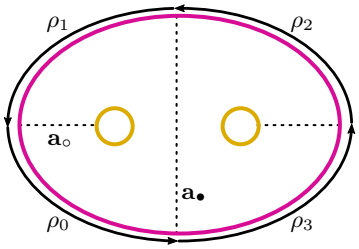

Figure 13. An arc system for the extended algebra $\widetilde{\mathcal{A}}$.

$$\rho_{i+1}\rho_i = 0$$

(indices interpreted modulo 4); see [13, Section 5.1] for a discussion of relations in surface algebras. Note that the products $\rho_i\rho_{i+1} = \rho_{i(i+1)}$ are non-zero. For consistency with [5, Section 3.1] we would need to add an additional relation $\rho_0\rho_1\rho_2\rho_3\rho_0 = 0$, but this is not necessary in the present setting.

The arc system associated with $\widetilde{\mathcal{A}}$ decomposes the torus into a single disk, so type D structures associated with compact train-tracks will be curved. We fix the curvature term $c = \rho_{0123} + \rho_{1230} + \rho_{2301} + \rho_{3012}$. Recall that a curved type D structure over $\widetilde{\mathcal{A}}$ satisfies the compatibility condition

$$(\mu \otimes \mathrm{id}_V) \circ (\mathrm{id}_{\widetilde{\mathcal{A}}} \otimes d) \circ d = c \cdot \mathrm{id}_{\widetilde{\mathcal{A}}}$$

and that, in this setting, the underlying $\mathbf{k}$-vector space decomposes so that $V = V_\bullet \oplus V_\circ$ as an $\mathcal{I}$-module.

The torus algebra is the quotient $\mathcal{A} = \widetilde{\mathcal{A}}/(\rho_0)$. Notice that in this quotient the curvature vanishes and the compatibility condition for type D structures given in Section 1 is recovered. This algebra is explored in depth in [16, Section 11] and in [5].

4 The proof of Theorem 2. We first provide a dictionary between the knot Floer structures used here and in [16]. Their filtered and associated graded complexes over $\mathbf{k}[u]$ are recovered from the type D structure invariant as follows:

$$CFK^-(S^3, K) = \mathbf{k}[u] \boxtimes \left({}^{\mathbf{k}[u,v]}\, CFK(S^3, K)\big|_{v=1} \right) \qquad gCFK^-(S^3, K) = \mathbf{k}[u] \boxtimes \left({}^{\mathbf{k}[u,v]}\, CFK(S^3, K)\big|_{v=0} \right)$$

The relationship between type D structures, modules, and filtered complexes is discussed in detail in [13, Section 3.2].

Given a type D structure ${}^{\mathcal{R}}CFK(S^3,K)$, we focus on the coefficient maps in each of the annuli A_v and A_u, and consider their images under the map $\frown$. The image of a map v^i is

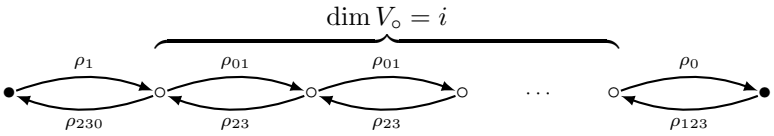

while the image of the map u^i is

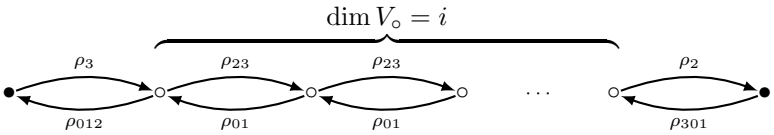

Passing to the quotient $\mathcal{A}$ by setting $\rho_0 = 0$ simplifies the above images to

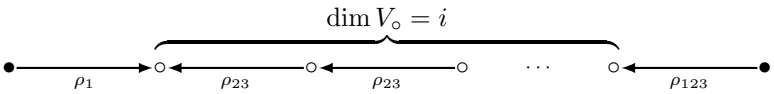

and

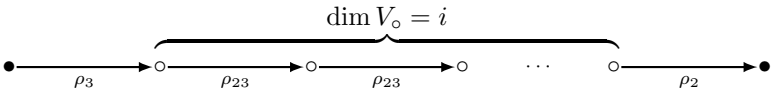

recovering the two *stable* chains appearing in the statement of [16, Theorem A.11].

The main subtlety is the appearance of the *unstable* chain, which we have already touched on. If we define $\frown$ in such a way that there is no extra twisting introduced (see the left of Figure 3), then joining the ends of the non-compact curve with a straight segment running over the handle adds a final map: 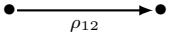 This is the unstable chain, identifying the distinguished generator of the vertical homology with that of the horizontal homology (each of which is a homology class for $\widehat{HF}(S^3) \cong \mathbf{k}$). This form of the unstable chain corresponds to the 2τ-framing of the knot K, as explained in [16, Theorem A.11]. The other choices of twisting in $\frown$ will result in the other presentations of the unstable chain. It follows that after identifying the once-punctured torus with the knot exterior (two cases are illustrated in Figure 3), the resulting curve on $\partial(S^3 \setminus \mathring{\nu}(K))$ is well-defined, and is equal to $\widehat{HF}(S^3 \setminus \mathring{\nu}(K))$.

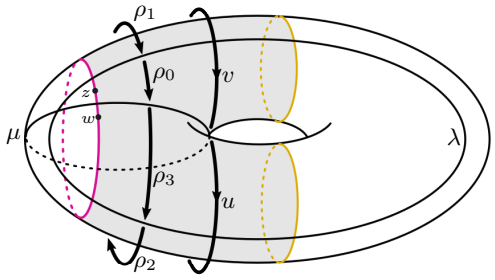

Figure 14. Both algebras $\mathcal{R}$ and $\widetilde{\mathcal{A}}$ in context.

We now consider how this process is reversed. Recall that, if $M = S^3 \setminus \mathring{\nu}(K)$, the homology $\widehat{HF}(S^3)$ is obtained from Lagrangian Floer homology $HF\big(\widehat{HF}(M),\mu\big)$ where μ is the knot meridian [5, Theorem 2]. Choose μ so that it passes between the basepoints z and w as in Figure 14, and consider the Lagrangian Floer complex $CF^z_{\not w}(\widehat{HF}(M),\mu)$ where discs covering w are blocked. It turns out that this recovers the knot Floer complex $gCFK^-(S^3,K)$ over $\mathbf{k}[u]$ [6, Theorem 51] or, equivalently, the horizontal type D structure $C^{\mathbf{h}}$. Analogously, blocking the discs covering z, the complex $CF^w_{\not z}(\widehat{HF}(M),\mu)$ recovers the vertical type D structure $C^{\mathbf{v}}$ over $\mathbf{k}[v]$. It follows from Proposition 4 that blocking only the discs that cover both z and w recovers the knot Floer type D structure over $\mathcal{R}$:

$$CF^{z,w}_{\not z\not w}(\widehat{HF}(M),\mu) \simeq {}^{\mathcal{R}}CFK(S^3,K)$$

The latter equivalence is also discussed in [4, Section 2.4]. It remains to note that the bigons involved in $CF^{z,w}_{\not z\not w}(\widehat{HF}(M),\mu)$ are precisely governed by segments of $\partial\mathcal{D}(\widehat{HF}(M))$ winding around

the punctures of the twice-punctured disk. Thus the operation $\cap$ takes the curve $\widehat{HF}(M)$ to the curve $\boldsymbol{\gamma}(K)$. □

5 Comments on generalizations and related work. Perhaps the most interesting step in this constructive review of the Lipshitz–Ozsváth–Thurston correspondence comes about when the endpoints of the non-compact component $\boldsymbol{\gamma}_0 \subset \boldsymbol{\gamma}$ are identified to give a new compact component in the once-punctured torus. Note that the output of $\cap$ is always a compact curve, and this is consistent with the observation that $\widehat{HF}(M)$ is a compact curve. The latter, in turn, follows from the fact that $\widehat{CFD}(M)$ is an extendable type D structure [5, Appendix A].

Joining the endpoints of the immersed curve $\boldsymbol{\gamma}_0$ associated with a knot K requires a choice of automorphism of $\mathbf{k}^n$ where n is the number of components in $\boldsymbol{\gamma}_0$. Denote the horizontal homology $H^{\mathbf{h}} = H_*(C^{\mathbf{h}}|_{u=1})$ and the vertical homology $H^{\mathbf{v}} = H_*(C^{\mathbf{v}}|_{v=1})$. Then in Theorem 2, because the knot is in S^3, it follows that $n = 1$ and the automorphism is given, tautologically, by

$$H^{\mathbf{v}}(CFK^-(S^3, K)) \cong H^{\mathbf{h}}(CFK^-(S^3, K)) \cong \widehat{HF}(S^3) \cong \mathbf{k}$$

as explained in [16, Section 11.5]. Thus, the operation $\cap$ is defined over any field, provided that we choose a coefficient $a \in \mathbf{k}$ with which we glue the ends of $\boldsymbol{\gamma}_0$ along a handle. We choose this coefficient to be $+1$ so that the bordered invariant for the solid torus is a circle with the trivial local system. We now note that bordered Floer homology is only defined over the two-element field $\mathbb{F}$. As such, the map $\cap$ and Theorem 2 gives a *candidate* bordered invariant for the knot exterior when $\mathbf{k} \neq \mathbb{F}$.

We now consider the general case of a knot K in Y. Decomposing along spin^c-structures, the same strategy as above works if Y is an L-space [9]. More generally, however, one needs to know the isomorphism

$$H^{\mathbf{v}}(CFK^-(Y, K)) \cong H^{\mathbf{h}}(CFK^-(Y, K)) \cong \widehat{HF}(Y)$$

(which may be block-decomposed according to spin^c-structures). This recovers a generalization of [16, Theorem A.11], which may be found in forthcoming work of Hockenhull [10] building on his invariant $\mathrm{Poly}(L, \Lambda)$ [11]. From our perspective, the passage from the knot Floer homology of a knot K in Y to the bordered invariants of $Y \setminus \mathring{\nu}(K)$ requires the isomorphism shown above. As there is a decomposition according to spin^c structure, there is no loss of generality in considering the case where Y is an integer homology sphere. When such a Y is not an L-space, we have that $\dim \widehat{HF}(Y) > 1$ and, in principle, the automorphism ψ induced by the isomorphism between the homologies $H^{\mathbf{h}}$ and $H^{\mathbf{v}}$ can be interesting. In particular, while all components of $\boldsymbol{\gamma}_0(K)$ carry trivial local systems, the new compact object $\cap(\boldsymbol{\gamma}_0(K))$ obtains an additional local system $(\mathbf{k}^n, \psi)$; see Figure 15. The key point of difference is that the output will be equivalent to a simply faced precurve (in the torus) in general, and a further application of the arrow sliding algorithm may be required to obtain immersed curves. The algebraic side of this story is laid out carefully by Hockenhull [10, 11].

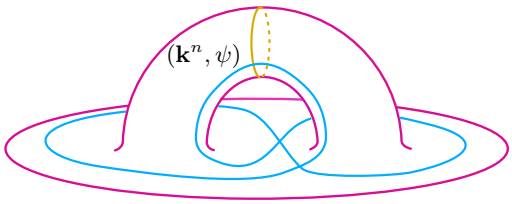

Figure 15. A sample hypothetical local system, where $n = \dim \widehat{HF}(Y)$.

Finally, Hanselman gives another approach [3]: His construction takes the complex $CFK^-(K)$ and outputs an immersed curve in the strip covering the twice-punctured disc D, containing a countable set of pairs of punctures. This cover of the disk is useful for recording the Alexander grading, and also works with general fields (hence producing candidate bordered invariants). We advertise that Hanselman's construction has a different aim in mind: His work gives a candidate bordered-minus invariant, by promoting the curves to describe type D structures over $\mathbf{k}[u, v]$.

6 The Proof of Theorem 3. For simplicity we first focus on the case of two-element field $\mathbf{k} = \mathbb{F}$. A few properties of invariant ${}^{\mathcal{R}}CFK(S^3, K)$ are needed for the proof. First, given two type D structures over the polynomial algebra $\mathbf{k}[u, v]$ or its quotient $\mathcal{R}$, their tensor product is another type D structure:

$$(V, d) \otimes (V', d') = (V \otimes_{\mathbf{k}} V', d \otimes \mathrm{id} + \mathrm{id} \otimes d').$$

Now, reformulating [17, Theorem 7.1] into a new language, the behavior of knot Floer homology under taking the connected sum can be described as follows:

$${}^{\mathcal{R}}CFK(S^3, K\#K') \simeq {}^{\mathcal{R}}({}^{\mathcal{R}}CFK(S^3, K) \otimes {}^{\mathcal{R}}CFK(S^3, K'))$$

The mirroring operation is also well understood [17, Proposition 3.7]:

$${}^{\mathcal{R}}CFK(S^3, \mathrm{m}K) \simeq {}^{\mathcal{R}}\overline{CFK(S^3, K)}$$

where the latter is the *dual type D structure*, equal to the original one but with all actions reversed [14, Definition 2.5] (since $\mathcal{R}$ is commutative, the fact that dualizing turns left type D structure to right ones is not a problem). At last, we need an algebraic relationship between morphism spaces of type D structures [15, Section 2.2.3] and their tensor products. Given any two type D structures, the definitions imply the following isomorphism of chain complexes:

$$\mathcal{R} \boxtimes {}^{\mathcal{R}}({}^{\mathcal{R}}\overline{N} \otimes {}^{\mathcal{R}}N') \cong \mathrm{Mor}({}^{\mathcal{R}}N, {}^{\mathcal{R}}N')$$

With the properties above in place, the proof of Theorem 3 is a sequence of isomorphisms:

$$\begin{aligned}
{}_{\mathcal{R}}HFK(S^3, \mathrm{m}K\#K') &\cong H_*(\mathcal{R} \boxtimes {}^{\mathcal{R}}CFK(S^3, \mathrm{m}K\#K')) \\
&\cong H_*(\mathcal{R} \boxtimes {}^{\mathcal{R}}[{}^{\mathcal{R}}CFK(S^3, \mathrm{m}K) \otimes {}^{\mathcal{R}}CFK(S^3, K')]) \\
&\cong H_*(\mathcal{R} \boxtimes {}^{\mathcal{R}}[{}^{\mathcal{R}}\overline{CFK(S^3, K)} \otimes {}^{\mathcal{R}}CFK(S^3, K')]) \\
&\cong H_*(\mathrm{Mor}({}^{\mathcal{R}}CFK(S^3, K), {}^{\mathcal{R}}CFK(S^3, K'))) \\
&\cong HF(\boldsymbol{\gamma}(K), \boldsymbol{\gamma}(K'))
\end{aligned}$$

where the final isomorphism follows from the general description of morphism spaces between type D structures over surface algebras [13, Theorem 1.5].

The recipe for adding signs follows the Koszul sign rule, which is discussed in [19, Section 12] in detail. We find that the resulting signs are a bit more more natural if one considers right type D structures [13, Example 2.10], rather than left ones [19, Section 12.3], as then there are no extra signs when box tensoring with $- \boxtimes_{\mathcal{R}} \mathcal{R}_{\mathcal{R}}$; this is explained in [13, Page 19]. Now, since the algebra $\mathcal{R}$ is commutative, our left type D structures can be viewed as right type D structures, and after that filling in the signs becomes straightforward. We refer the reader to [13, Sections 2 and 5]. □

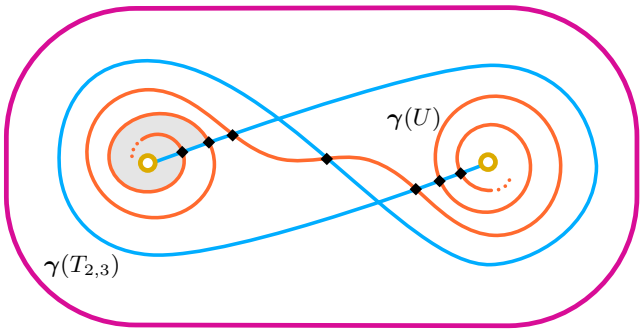

Figure 16. Illustrating Theorem 3 in the case of the unknot $K = U$ and the right-hand trefoil $K' = T_{2,3}$. The curve $\boldsymbol{\gamma}(U)$ is a horizontal arc connecting the punctures, but because we are in the wrapped setting, one needs to wrap $\boldsymbol{\gamma}(U)$ infinitely many times around the punctures when pairing with another curve.

To illustrate this gluing result, suppose $K = U$ and $K' = T_{2,3}$. Then the knot Floer homology of the connected sum is equal to

$$\mathcal{R}HFK(S^3, T_{2,3}) = H_*(\mathcal{R} \xleftarrow{\cdot v} \mathcal{R} \xrightarrow{\cdot u} \mathcal{R}) = [\cdots \xleftarrow{v} \blacklozenge \xleftarrow{v} \blacklozenge \xleftarrow{v} \blacklozenge \xrightarrow{u} \blacklozenge \xleftarrow{v} \blacklozenge \xrightarrow{u} \blacklozenge \xrightarrow{u} \blacklozenge \xrightarrow{u} \cdots]$$

where the arrows indicate the $\mathcal{R}$-action. The corresponding wrapped Lagrangian Floer homology $HF(\boldsymbol{\gamma}(U), \boldsymbol{\gamma}(T_{2,3}))$ is illustrated in Figure 16. Note that in this example the $\mathcal{R}$-action can be seen geometrically by counting Maslov index 2 discs covering the punctures; one of these is shaded in the picture. The same is true for $\mathbf{k}[H]$-action on Bar-Natan homology, viewed as wrapped Lagrangian Floer homology of immersed curves in [13, Example 7.7]. In general, to recover these module-structures, only some of the Maslov index 2 discs should be counted—we will investigate this in a future work.

Acknowledgements. This short paper benefited from stimulating conversations with Jonathan Hanselman, Thomas Hockenhull, and Matthew Stoffregen. The work was initiated during the CRM50 thematic program *low dimensional topology* and we thank the CRM and CIRGET for hosting a great event.

References

[1] I. Dai, J. Hom, M. Stoffregen, and L. Truong. More concordance homomorphisms from knot Floer homology, 2019. ArXiv preprint 1902.03333.
[2] F. Haiden, L. Katzarkov, and M. Kontsevich. Flat surfaces and stability structures. *Publ. Math. Inst. Hautes Études Sci.*, 126:247–318, 2017. (ArXiv: 1409.8611).
[3] J. Hanselman. Knot Floer homology via immersed curves. In preparation.
[4] J. Hanselman. Heegaard Floer homology and cosmetic surgeries in S^3, 2019. ArXiv preprint 1906.06773.
[5] J. Hanselman, J. Rasmussen, and L. Watson. Bordered Floer homology for manifolds with torus boundary via immersed curves, 2016. ArXiv preprint 1604.03466.
[6] J. Hanselman, J. Rasmussen, and L. Watson. Heegaard Floer homology for manifolds with torus boundary: properties and examples, 2018. ArXiv preprint 1810.10355.
[7] J. Hanselman and L. Watson. Cabling in terms of immersed curves, 2019. ArXiv preprint 1908.04397.
[8] M. Hedden, C. M. Herald, and P. Kirk. The pillowcase and perturbations of traceless representations of knot groups. *Geom. Topol.*, 18(1):211–287, 2014. (ArXiv: 1301.0164).
[9] M. Hedden and A. S. Levine. Splicing knot complements and bordered Floer homology. *J. Reine Angew. Math.*, 720:129–154, 2016. (ArXiv: 1210.7055).
[10] T. Hockenhull. Duality patterns in knot Floer homology. In preparation.
[11] T. Hockenhull. Holomorphic polygons and the bordered Heegaard Floer homology of link complements, 2018. ArXiv preprint 1802.02443.
[12] J. Hom. *Heegaard Floer Invariants and Cabling*. ProQuest LLC, Ann Arbor, MI, 2011. Thesis (Ph.D.)–University of Pennsylvania, (https://repository.upenn.edu/edissertations/329/).
[13] A. Kotelskiy, L. Watson, and C. Zibrowius. Immersed curves in Khovanov homology, 2019. ArXiv preprint 1910.14584.
[14] R. Lipshitz, P. S. Ozsváth, and D. P. Thurston. Heegaard Floer homology as morphism spaces. *Quantum Topol.*, 2(4):381–449, 2011. (ArXiv: 1005.1248).
[15] R. Lipshitz, P. S. Ozsváth, and D. P. Thurston. Bimodules in bordered Heegaard Floer homology. *Geom. Topol.*, 19(2):525–724, 2015. (ArXiv: 1003.0598).
[16] R. Lipshitz, P. S. Ozsváth, and D. P. Thurston. Bordered Heegaard Floer homology. *Mem. Amer. Math. Soc.*, 254(1216):viii+279, 2018. (ArXiv: 0810.0687).
[17] P. S. Ozsváth and Z. Szabó. Holomorphic disks and knot invariants. *Adv. Math.*, 186(1):58–116, 2004. (ArXiv: math/0209056).
[18] P. S. Ozsváth and Z. Szabó. Algebras with matchings and knot Floer homology. 2019. ArXiv preprint 1912.01657.
[19] P. S. Ozsváth and Z. Szabó. Bordered knot algebras with matchings. *Quantum Topol.*, 10(3):481–592, 2019. (ArXiv: 1707.00597).
[20] J. Rasmussen. *Floer homology and knot complements*. ProQuest LLC, Ann Arbor, MI, 2003. Thesis (Ph.D.)–Harvard University, (ArXiv: math/0306378).
[21] I. Zemke. Connected sums and involutive knot Floer homology. *Proc. Lond. Math. Soc. (3)*, 119(1):214–265, 2019. (ArXiv: 1705.01117).
[22] C. Zibrowius. Peculiar modules for 4-ended tangles. *J. Topol.*, 13(1):77–158, 2020. (ArXiv: 1712.05050).

Department of Mathematics, Indiana University

Email address: artofkot@iu.edu

Department of Mathematics, University of British Columbia

Email address: liam@math.ubc.ca

Department of Mathematics, University of British Columbia

Email address: claudius.zibrowius@posteo.net